Supporting Information

Sustainable Lignin-Based Ionic Hydrogel for High-Performance Moisture-Electric Generation and Self-Powered Wearable Sensing

Xinli Tang [a], Yijun Lu [b], Qiang Shi [a], Hongfeng Yu [b], Xiaoliang Ren [b], Dayong Zheng [c], Jianqiang Xie [a], Jiankui Sun [a]*

Experimental Section

Synthesis of the EHL-Al^{3+}-PAA Ionic Hydrogel

Table S1 Different Al^{3+} for the hydrogel preparations

EHL (g)	$AlCl_3 \cdot 6H_2O$ (g)	AA (g)	APS (g)	Water (g)	EG (g)
0.15	0.8	2	0.03	4	2.5
0.15	1.0	2	0.03	4	2.5
0.15	1.2	2	0.03	4	25
0.15	1.5	2	0.03	4	2.5
0.15	1.8	2	0.03	4	2.5

Table S2 Different EHL for the hydrogel preparations

EHL (g)	$AlCl_3 \cdot 6H_2O$ (g)	AA (g)	APS (g)	Water (g)	EG (g)
0.15	1.2	2g	0.03	4	2.5
0.2	1.2	2g	0.03	4	2.5
0.25	1.2	2g	0.03	4	25
0.3	1.2	2g	0.03	4	2.5
0.35	1.2	2g	0.03	4	2.5

Table S3 Electrical properties of different electrodes

EHL (g)	$AlCl_3 \cdot 6H_2O$ (g)	AA (g)	APS (g)	Water to EG (g)
0.15	0.8	2g	0.03	6:0
0.15	1.0	2g	0.03	5:1.5
0.15	1.2	2g	0.03	4:2.5
0.15	1.5	2g	0.03	3.5:3
0.15	1.8	2g	0.03	1.5:5

Table S4 The ratio of glycol to water of EHL-Al^{3+}-PAA hydrogels

Electrode Types (Positive/Negative)	Open-circuit voltage(V)	Open-circuit current(μA)
Carbon cloth/Carbon cloth	0.85	1
Carbon cloth/Copper plate	0.84	253
Carbon cloth/Aluminium plate	1.22	1410
Carbon cloth/Zinc plate	1.61	1945

Table S5 Comparison of reported hydrogel-based HMEGs with our study

Functional layer	Size (cm^2)	Current (μA)	Voltage (V)	Electrode Type (Positive+ Negative)	Reference
PVA-PAn-GI-GC	0.25	102.8	0.58	Carbon tape+Zn@NiO@/ZnO@ C_3N_4	[1]
BPFs	0.25	5	0.95	a pair of inert conductive CT electrodes	[2]
rGO/GO	3.14	0.038	1.5	Au+Ag	[3]
HL-EL	1	100	1.4	Carbon slurry+Zn powde	[4]
PVA/PNIPAM	1	33.23	0.34	Carbon Cloth+Carbon Cloth	[5]
PVA/AlgNa/$CaCl_2$	1	2100	1.3	Graphene+Aluminum electrode	[6]
PSS/GO/GI/PVA	1	7.08	0.55	LM/C+Ag	[7]
MEH	1	480	0.81	Ag+Pt	[8]
DESL–Al^{3+}–PAA	1	22.37	1.32	Carbon+Aluminum electrode	[9]
LS-H	0.25	1200	1.26	Carbon+Zn	[10]
LS–Al^{3+}–PAA	1	3.28	0.55	Ag+Carbon	[11]
PEDOT/PSS/PA-Wood	1	360	0.73	Cu+copper grids	[12]
PGHEG(LS-QC)	1	---	0.13	Zn and graphite paper electrodes	[13]
LS-g-PAA-Al	4	---	0.15	Ti mesh+Carbon cloth (CC)	[14]
EHL-Al^{3+}-PAA	**1**	**4000**	**1.71**	**Carbon+Zn**	**This work**

Characterization and Measurements

Adhesion Performance Tests Tensile bonding tests were used to evaluate the adhesive properties of hydrogels to a variety of substrates, including glass, pigskin, PTFE, zinc, and metal. To minimize experimental error, five parallel samples were taken for each experiment. Briefly, a 2 mm thick layer of hydrogel was applied to the surface of the substrate with a bonding area of 25 mm × 25 mm, and then the specimens were subjected to tensile tests using a universal testing machine (Shimadzu Corporation, Japan) at a beam speed of 50 mm/min until failure. The bond strength was calculated by dividing the maximum load by the bond area. Self-healing performance was tested mainly by observing the self-healing time of the EHL-Al^{3+}-PAA hydrogel cut in half at 25°C.

Conductivity of measurement of the hydrogel The ionic conductivity of the hydrogel electrolyte was measured using the electrochemical impedance method on a CHI760E electrochemical workstation (Chenhua, Shanghai, China). To measure the conductivity the applied voltage and measuring frequency were maintained 1 V and 1 kHz, respectively. The conductivity was calculated by the following equation:

$$\sigma(S/cm) = \frac{L}{R \cdot A}$$

R is the intersection of the curve in the high-frequency region (left side) with the horizontal axis in the eis plot (Z' on the horizontal axis and -Z'' on the vertical axis)

L is the thickness of the hydrogel

A is the contact area of the electrodes with the sample

Flexible Sensing Testing The sensing characteristics were investigated using the amperometric i-t curve of the electrochemical workstation. The strain factor (GF) was calculated by the following equation. Where R is the real-time resistance of the hydrogel and R_0 is the initial resistance. ε is the strain applied when the hydrogel is stretched.

$$\mathrm{GF} = \frac{(R - R_0)/R}{\varepsilon} = \frac{\Delta R/R_0}{\varepsilon}$$

Results and Discussion

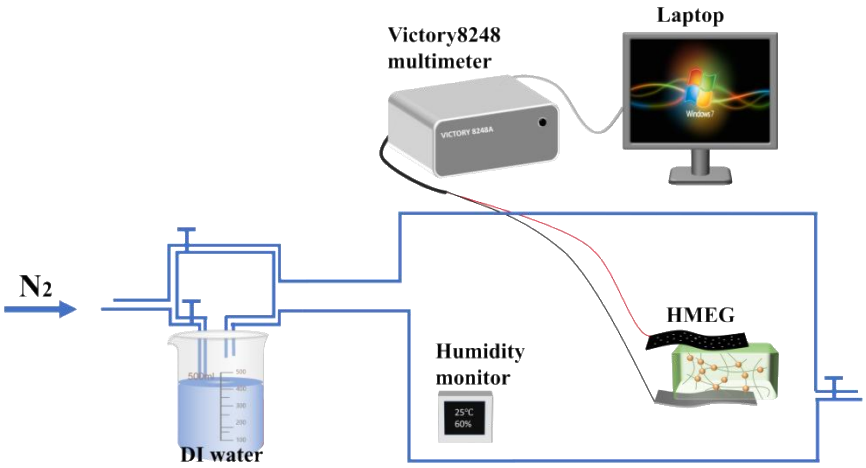

Fig. S1 Controlling relative humidity through adjustment of nitrogen flow rate.

Fig. S2 Digital photographs of solution systems without radical scavenger, with partial radical scavenger (isopropanol), and with complete radical scavenger (KI).

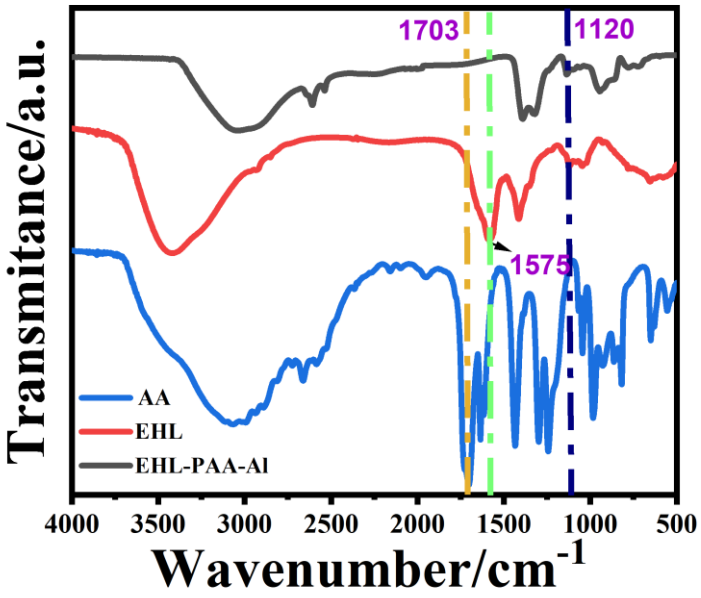

Fig. S3 the FTIR spectra of EHL, AA, and hydrogel

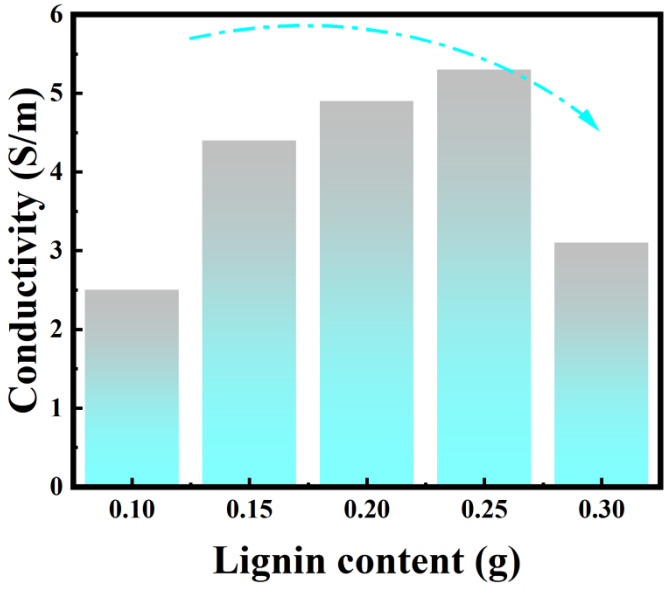

Fig. S4 Conductivity diagram at different EHL concentrations.

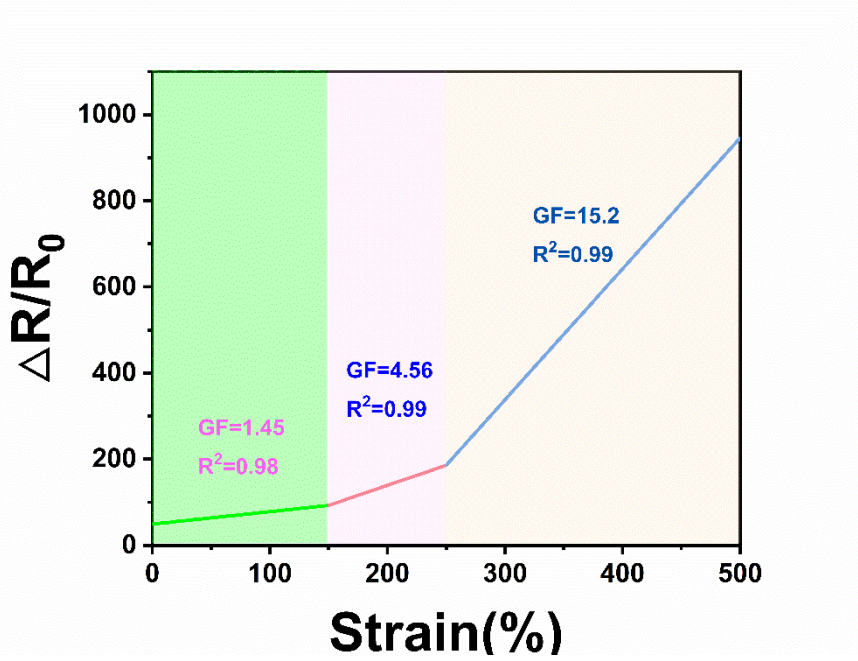

Fig. S5 Testing of hydrogels for electrical conductivity and flexible sensing properties: GF value of hydrogel at 0-500% stretch.

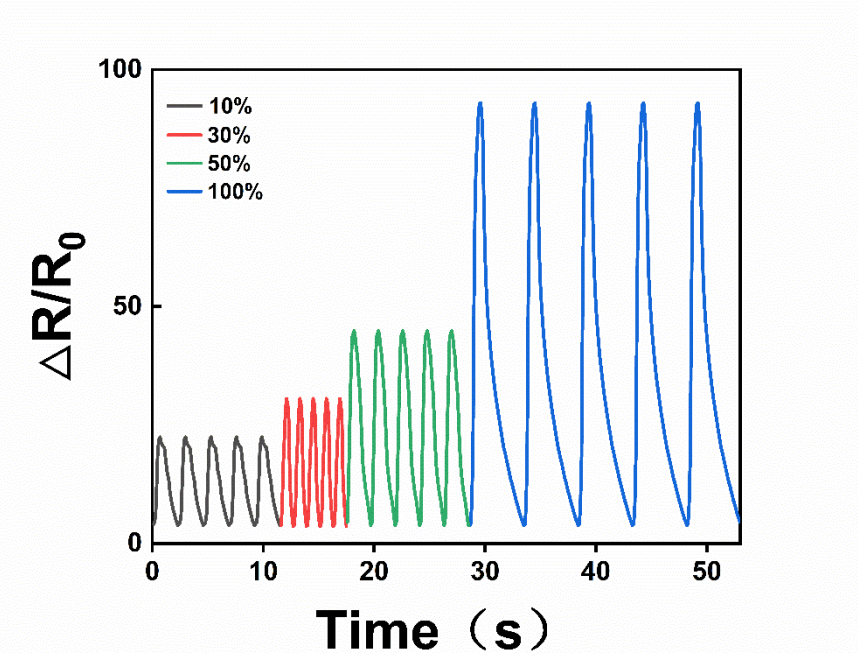

Fig. S6 Testing of hydrogels for electrical conductivity and flexible sensing properties: Relative resistance change curves of hydrogel at 10%, 30%, 50%, and 100% stretch.

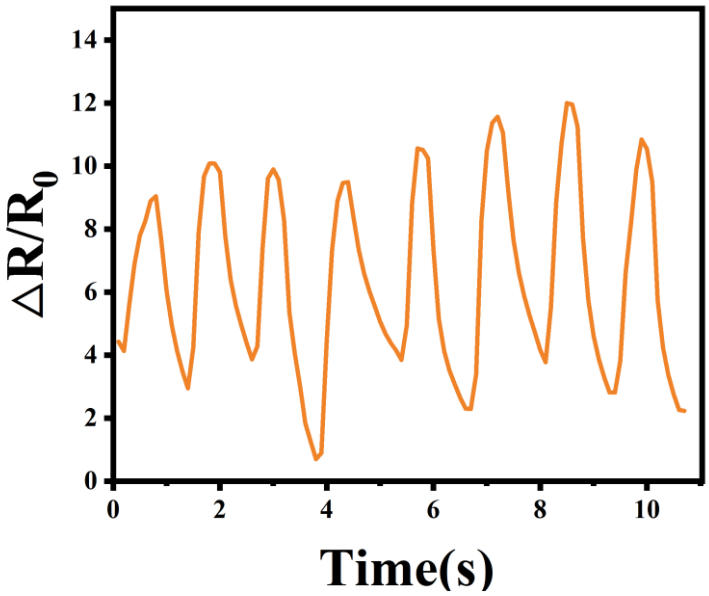

Fig. S7 Relative resistance change of hydrogel flexible sensors with knuckle flexion.

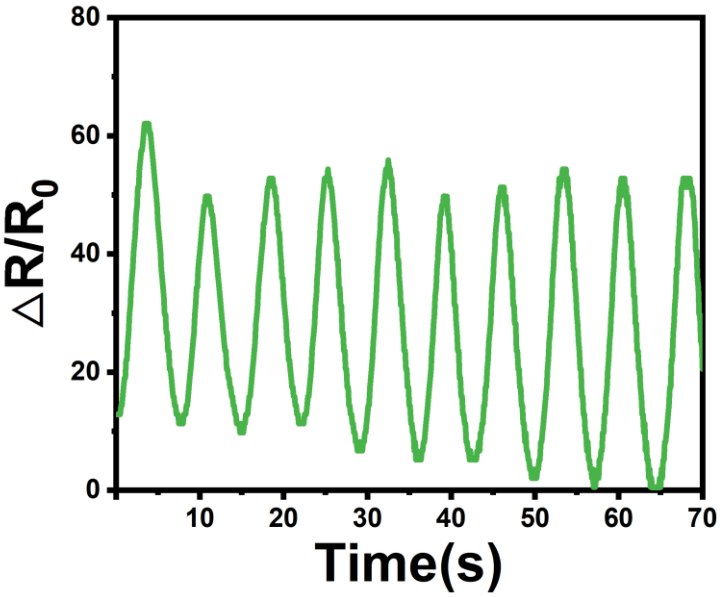

Fig. S8 Relative resistance change of hydrogel flexible sensors with wrist flexion.

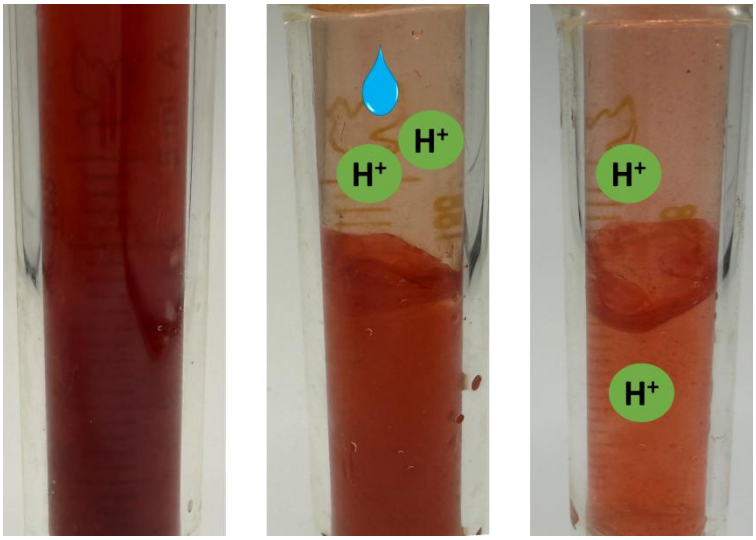

Fig. S9 Visualization experiment of hydrogen ion diffusion and migration. The EHL-Al^{3+}-PAA hydrogel is sandwiched between two syringe tubes containing methyl orange solution.

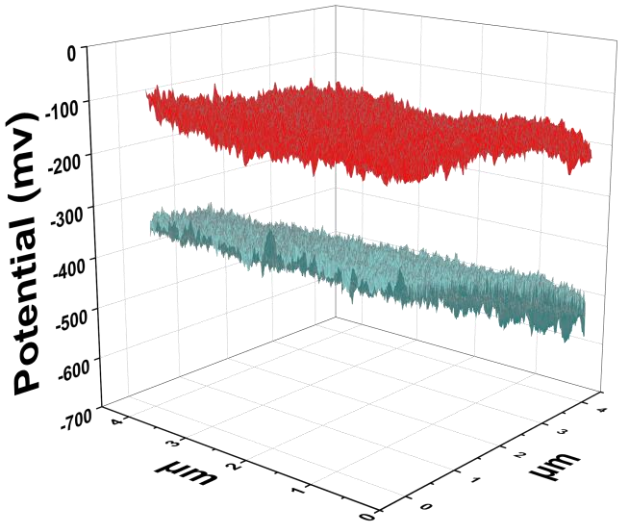

Fig. S10 Changes in surface potential of the hydrogel before moisture absorption (blue) and after 20 minutes of moisture absorption (red).

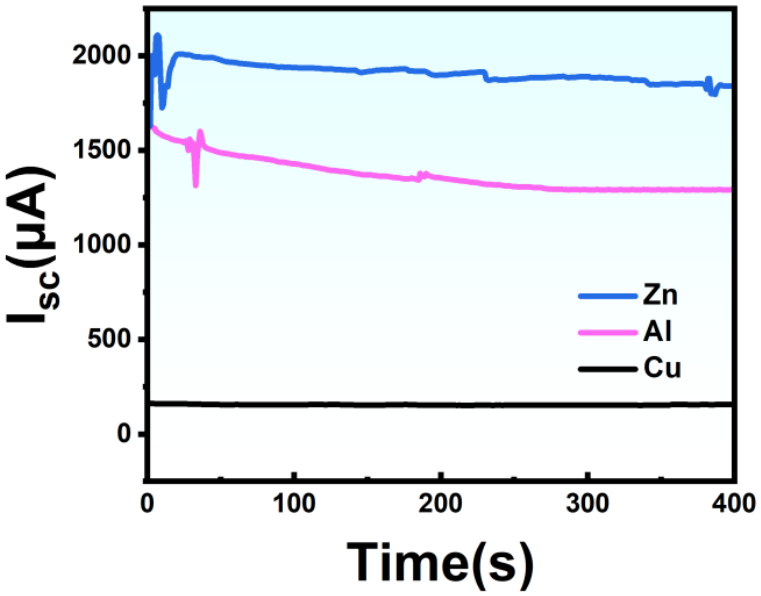

Fig. S11 Current output performance of copper, aluminium and zinc electrodes.

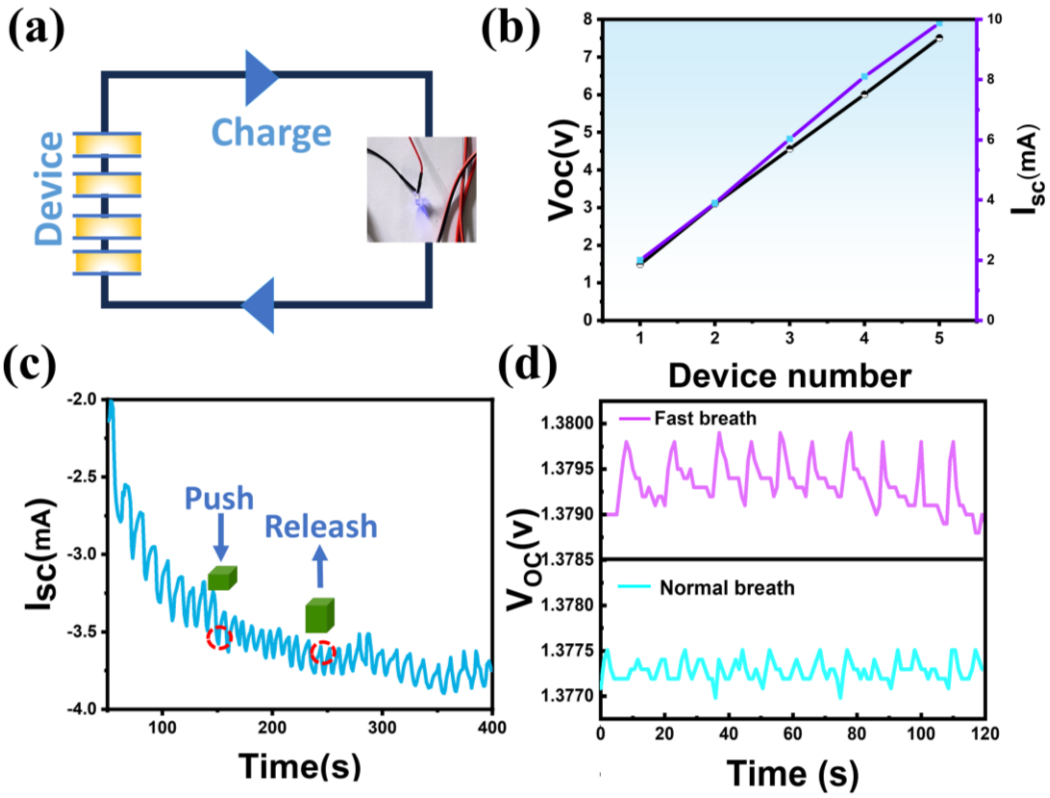

Fig. S12 Integration and application of the HMEG device. (a) Schematic illustration of the device integration structure. (b) Electrical output performance of the integrated device. (c) Output signal of the self-powered sensor based on the HMEG. (d) Demonstration of the device for respiratory monitoring.

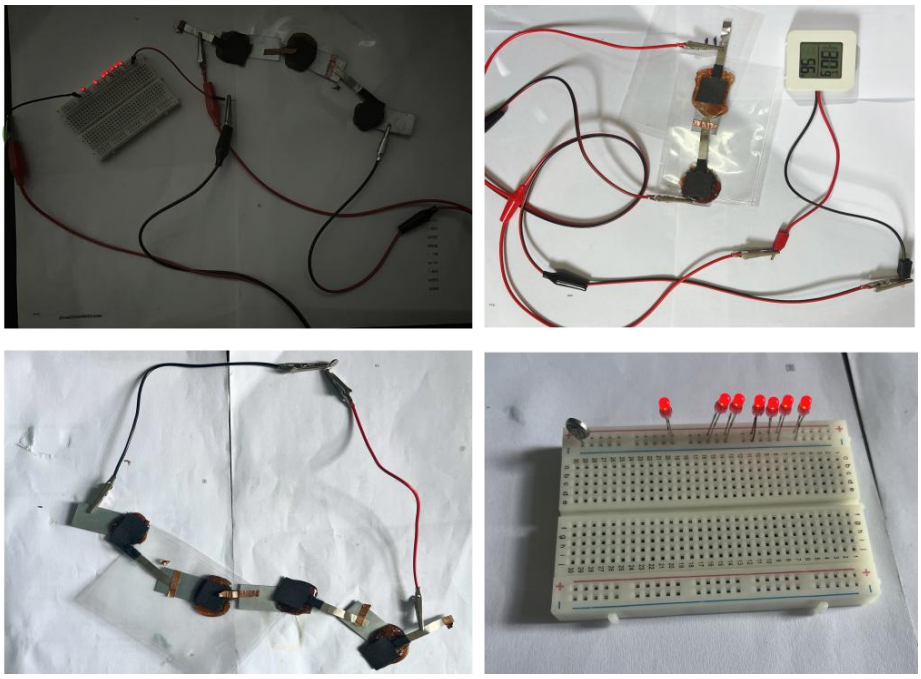

Fig. S13 The moisture-powered machine consists of a row of light bulbs, a temperature and humidity display, and a capacitor charger.

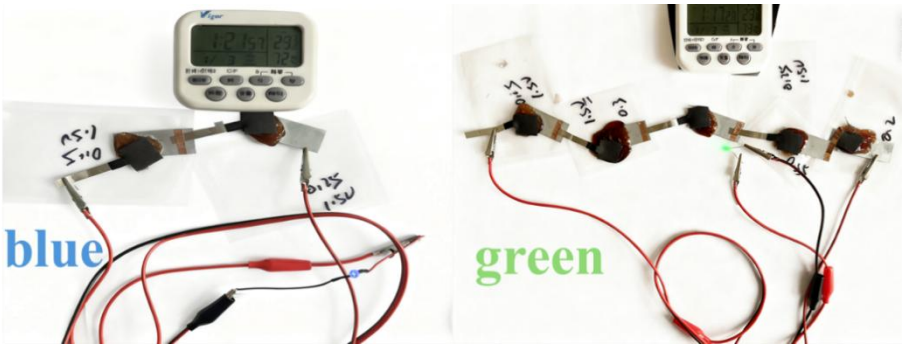

Fig. S14 Two devices can light a small bulb for dozens of days.

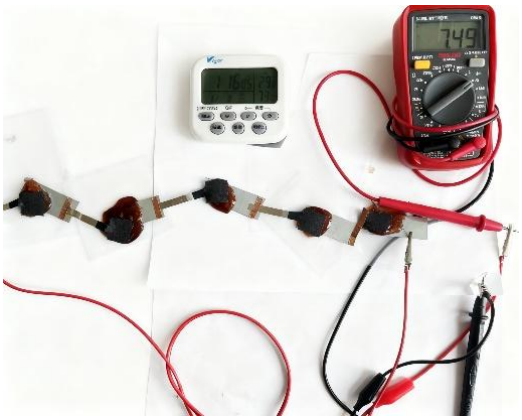

Fig. S15 Voltage values for five devices at room temperature (26°C) and humidity (70%).

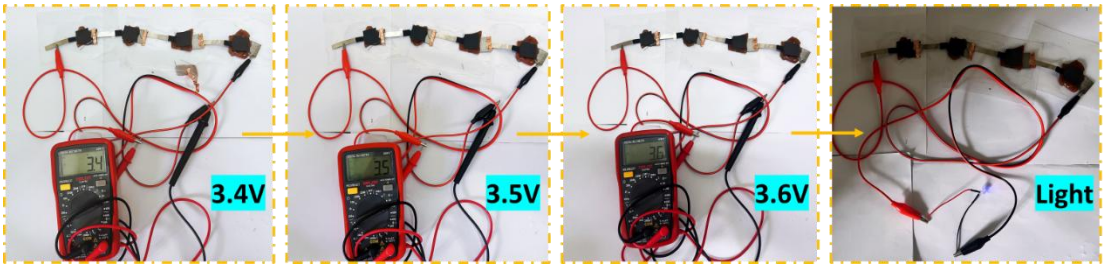

Fig. S16 Voltage changes and lighting of LED bulbs in four HMEG devices at room temperature of 26 degrees Celsius and humidity Rh=60% conditions.

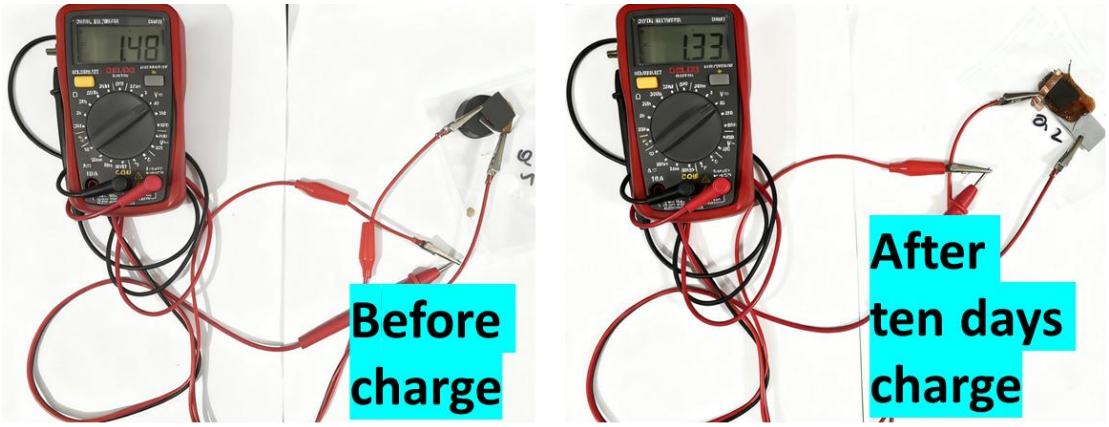

Fig. S17 Voltage change after ten days of charging a light bulb by a moisture generator.

References

1. F. Yu, L. Wang, X. Yang, Y. Yang, X. Li, Y. Gao, Y. Jiang, K. Jiang, W. Lu and X. Sun, *ACS Nano*, 2025, **19**, 3807-3817.
2. H. Wang, Y. Sun, T. He, Y. Huang, H. Cheng, C. Li, D. Xie, P. Yang, Y. Zhang and L. Qu, *Nat. Nanotechnol.*, 2021, **16**, 811-819.
3. Y. Huang, H. Cheng, C. Yang, P. Zhang, Q. Liao, H. Yao, G. Shi and L. Qu, *Nat. Commun.*, 2018, **9**, 4166.
4. Y. Chen, C. Ye, J. He, R. Guo, L. Qu and S. Tang, *Energy Environ. Sci.*, 2025, **18**, 6063-6075.
5. G. Ma, W. Li, X. Zhou, X. Wang, M. Cao, W. Ma, J. Wang, H. Yu, S. Li and Y. Chen, *ACS Appl. Polym. Mater.*, 2024, **6**, 7066-7076.
6. S. Yang, L. Zhang, J. Mao, J. Guo, Y. Chai, J. Hao, W. Chen and X. Tao, *Nat. Commun.*, 2024, **15**, 3329.
7. Y. Liu, Z. Li, X. Yang, Y. Yang, X. Li, Y. Jiang, Y. Gao, L. Wang and W. Lü, *Adv. Funct. Mater.*, 2024, **34**, 2407204.
8. H. Zhang, N. He, B. Wang, B. Ding, B. Jiang, D. Tang and L. Li, *Adv. Mater.*, 2023, **35**, 2300398.
9. Z. Liu, Y. Hou, L. Lei and S. Hu, *J. Mater. Chem. A*, 2024, **12**, 9701-9713.
10. S. You, M. Chen, H. Ren, L. Zhu, P. Wang, W. Sheng and W. Li, *ACS Appl. Mater. Interfaces*, 2025, **17**, 12034-12042.
11. J. Zhang, J. Zhuang, L. Lei and Y. Hou, *J. Mater. Chem. A*, 2023, **11**, 3546-3555.
12. T. Zhang, X. Han, Y. Peng, H. Yu and J. Pu, *Polymers*, 2024, **16**, 260.
13. X. Pan, Q. Wang, D. Benetti, L. Jin, Y. Ni and F. Rosei, *J. Mater. Chem. A*, 2023, **11**, 19506-19513.
14. A. K. Mondal, D. Xu, S. Wu, Q. Zou, W. Lin, F. Huang and Y. Ni, *Int. J. Biol. Macromol.*, 2022, **207**, 48-61.